THE JOURNAL OF PHYSICAL CHEMISTRY A
A JOURNAL OF THE AMERICAN CHEMICAL SOCIETY

pubs.acs.org/JPCA Article

Structures and Electron Affinities of Aluminum Hydride Clusters Al_nH (n = 3−13)

John C. Poutsma,* William Moeller, Jennifer L. Poutsma, Brendan C. Sweeny, Shaun G. Ard, Albert A. Viggiano, and Nicholas S. Shuman

Cite This: J. Phys. Chem. A 2022, 126, 1648−1659 Read Online

ABSTRACT: Low-energy structures and electron affinities (EAs) for aluminum hydride clusters Al_nH (n = 3−13) have been calculated using *ab initio* and density functional calculations. Geometries were optimized at the PBE0/def-2-TZVPP level of theory, which has been shown to match the currently accepted lowest-energy structures for the all-aluminum clusters Al_n and their anions. Neutral hydride clusters with n = 4, 7, and 9−12 are predicted to adopt terminal structures with the hydrogen atom bound to only one aluminum atom and with only minor alterations of the aluminum atom arrangement from that of the all-aluminum cluster. Clusters with n = 3 and 13 are predicted to adopt "face-centered" geometries, and the n = 6 cluster is predicted to prefer an isomer with the hydrogen atom bridging two aluminum atoms, also with little or no distortion to the aluminum atom arrangement from the all-aluminum cluster. Addition of a hydrogen atom to clusters with n = 5 and 8 is predicted to distort the aluminum atom arrangement significantly from that of the corresponding all-aluminum cluster. In the anionic clusters, terminal clusters are preferred for all cluster sizes except for n = 6 that prefers a face-centered arrangement. Minor distortions in the aluminum scaffolding for Al_{11} and Al_{12} were found, while all other anionic clusters adopt structures with little or no deviation in the aluminum atom arrangement from the corresponding all-aluminum cluster. Raw adiabatic electron affinities were computed using CCSD(T)/aug-cc-pVTZ single-point energies for the anionic and neutral hydride clusters at their respective DFT geometries. Isodesmic electron affinities for the hydride clusters were computed relative to their all-aluminum counterparts and show an even-odd alternation with cluster size. Derived EAs alternate in magnitude between even- and odd-numbered clusters, with the even-numbered clusters having relatively larger EAs.

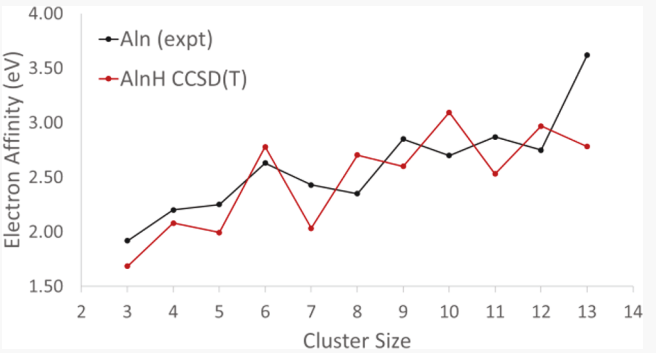

INTRODUCTION

Aluminum is of interest as a potential energy storage medium and fuel additive, but its facile reaction with molecular oxygen in the bulk phase hampers its utility. Early work by Jarrold et al.[1] and Castleman[2] and co-workers showed that certain small aluminum cluster ions (Al_7^+, Al_{13}^-, and Al_{23}^-) were resistant to reaction with molecular oxygen. These "magic number" clusters are consistent with closed-shell species from the so-called "jellium" model that treats the cluster nuclei as a united atom with a corresponding number of s and p valence electrons.[3] The magic number cluster ions have 20, 40, and 70 electrons. Interestingly, Castleman and co-workers also noted that there was an even-odd variation with cluster size in the efficiencies of the reaction in both the cationic and anionic clusters.[2] For example, in Al_n^- clusters, even-numbered clusters react more favorably than odd-numbered clusters. Since odd-numbered cluster anions are ground-state singlets, the reaction with triplet oxygen molecules is formally spin-forbidden, and this was thought to be the cause for the decrease in reaction rates.[2] Burgert et al. presented results also implicating spin conservation in the differing reactivity of these clusters.[4] By examining the reactivity of Al_nH^- clusters, which have an additional electron, they showed that the even-odd reactivity trend was reversed. That is, odd-numbered Al_nH^- clusters reacted more favorably.[4]

In recent work from our laboratory, we studied the temperature dependence of the reactions of aluminum cluster anions Al_n^- (n = 3−17) with molecular oxygen allowing us to determine Arrhenius parameters for the reactions.[5] Interestingly, the pre-exponential factors $k_{pre,}$ which correspond to the rate constants at infinite temperature, were found to decrease as a function of n^{-1} for both the even and the odd clusters, suggesting a similar mechanism. In addition, the pre-

Received: December 9, 2021
Revised: February 24, 2022
Published: March 4, 2022

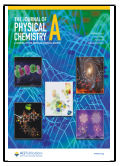

https://doi.org/10.1021/acs.jpca.1c10431
J. Phys. Chem. A 2022, 126, 1648−1659

exponential factors for the odd clusters were found to be a factor of ∼3 times larger than those for the even clusters despite their slower overall rates at room temperature. The difference in k_{pre} can be rationalized by a proposed mechanism in which the first step is electron transfer from the cluster anion to the O_2 molecule, similar to oxidation of an aluminum surface.[6,7] Transfer of an electron from a ground-state singlet odd-numbered cluster anion to O_2 results in a reactive triplet surface. In contrast, electron transfer from a ground-state doublet even-numbered cluster anion can result in either a reactive doublet surface or an unreactive quartet surface. Under spin-conservation, electron transfer on the adiabatic doublet surface can proceed on a surface diabatically correlated to $^1Al_n + {}^2O_2^-$, while electron transfer on a quartet surface must reach a potential diabatically correlated to excited state $^3Al_n + {}^2O_2^-$, resulting in a larger energetic barrier and greatly diminished reactivity for the quartet. Thus, the even-numbered cluster anion reactivity is decreased by a factor of ∼3. This implies that the spin constraint is actually for the even-numbered clusters (doublets) rather than for the odd-numbered clusters (singlets), in contrast to the proposed mechanism based on room temperature kinetics data. Given that the rate-limiting step in the proposed mechanism is an initial electron transfer from the cluster anion to O_2, we postulated that the experimentally-derived activation barriers should track the experimental electron affinities of the clusters. This was indeed the case for aluminum clusters with $n > 9$.[5]

Addition of a single hydrogen atom to the cluster anions causes a change in spin with the even-numbered hydride clusters having doublet ground states and the odd-numbered hydride clusters having singlet ground states. Previous room temperature studies of the reactivity of Al_nH^- with molecular oxygen also showed an even-odd alternation of the rate constant with the odd clusters reacting faster than the even clusters.[4] These studies were originally used as further proof of the spin conservation effect. In our recent work, we also measured temperature-dependent rate constants for reactions of five Al_nH^- cluster anions (n = 3, 4, 10, 11, and 12) with oxygen.[5] The results pointed to a similar mechanism to that for the all-aluminum clusters: odd clusters react faster than even clusters, even clusters have larger k_{pre} than odd clusters, and even clusters have larger activation barriers than odd clusters.[5] These results suggested that the reactivity should also track the electron binding energy of the Al_nH^- clusters. Experimental electron affinities were not available for the aluminum hydrides, so we calculated them using coupled-cluster single-point energies at density functional theory-derived geometries: CCSD(T)/aug-cc-pVTZ//PBE0/def2-TZVPP. Preliminary estimates for adiabatic electron affinities were calculated for hydride clusters with 3, 4, 10, 11, and 12 aluminum atoms using isodesmic calculations with the corresponding all-aluminum clusters serving as the reference. As for the all-aluminum clusters, for $n > 9$, the experimentally derived activation barriers for the reaction of the hydride clusters with O_2 were found to track the computed electron affinity of the cluster. In preparation for additional studies of Al_nH^- reactivity studies, we decided to carry out a more detailed study of the calculated low-energy structures and electron affinities for aluminum hydride clusters (n = 3−13), the results of which are presented here.

COMPUTATIONAL METHODS

All calculations were performed using either the Gaussian 09[8] or Gaussian 16[9] suite of programs. For geometry optimizations, restricted calculations were used for all ground-state singlet molecules and unrestricted calculations were used for all ground-state doublet molecules. For CCSD(T) single-point energy calculations,[10] we used restricted calculations for ground-state singlet molecules and restricted-open-shell calculations for ground-state doublet molecules due to an unreasonable amount of spin-contamination in the unrestricted Hartree−Fock (UHF) wave function used for generating CCSD configurations. Relative energetics are presented by comparing 0 K energies obtained from adding the zero-point vibrational energy calculated from unscaled harmonic vibrational frequency calculations to the total electronic energy obtained from single-point energy calculations performed at the minimized geometry.

Geometry Optimizations. The lowest energy geometries for neutral, anionic, and cationic aluminum clusters up to n = 13 have been established using a variety of techniques, including genetic algorithm tight-binding calculations,[11] genetic algorithm basin hopping methods,[12] and quantum Monte Carlo methods,[13] to sort through the various low-energy structures followed by density functional theory calculations for geometry optimizations. The hybrid-generalized gradient approximation (hybrid-GGA) density functional method PBE0 has been used in numerous studies for final geometry optimization based on recommendations by Chuang et al.,[11] Ahlrichs and Drebov,[12] Kiohara et al.,[14] and Paranthaman et al.[15] A recent study by Paranthaman et al. showed that single-point energy calculations at the PBE0/def2-TZVPP geometries gave energetic parameters including vertical and adiabatic electron affinities that were in close agreement with experimental and higher-level theoretical studies.[15] We chose to use this geometry optimization method for the Al_nH and Al_nH^- clusters based on its performance with the all-aluminum clusters.

Aluminum clusters Al_n and Al_n^- (n = 3−13) were re-optimized at the PBE0/def2-TZVPP level[16,17] using the structures and symmetries available in the literature as starting points.[11−13,18] Final geometries and symmetries were in agreement with published data from Chuang et al.,[11] Drebov and Ahlrichs,[12] Candido et al.,[13] Kiohara et al.,[14] and Paranthaman.[15] These cluster geometries were also used for CCSD(T) single-point energy calculations[10] that were then used for isodesmic calculations of the adiabatic electron affinities of the hydride clusters (see below). We also used the PBE0 structures for the all-aluminum clusters as starting points for determining low-energy isomers for the hydride clusters. Candidate structures for the singly hydrated clusters were generated by adding a hydrogen atom to each symmetry-unique terminal atom of the corresponding all-aluminum cluster. Additional candidate structures were generated with hydrogen atoms occupying symmetry-unique "face" and "edge (bridge)" positions of the clusters. Initial geometry screening of candidate structures was carried out at the PBE0/def2-TZVPP level for Al_nH/Al_nH^- with $n \leq 9$ and at PBE0/3-21G[19] level of theory for $n > 9$. Several of the low-lying isomers for the larger clusters were then re-optimized at the PBE0/def2-TZVPP level of theory. Frequency calculations were carried out for each conformer to ascertain whether the structure was a minimum or a transition state. Any transition states were

https://doi.org/10.1021/acs.jpca.1c10431
J. Phys. Chem. A 2022, 126, 1648−1659

subjected to intrinsic reaction coordinate (IRC) calculations, and the calculated minima were re-optimized, albeit under lower symmetry conditions. At the request of a reviewer, we investigated several other geometry optimization methods for Al_3/Al_3H and their anions including B3LYP[20,21]/def2-TZVPP, M06-2X[22]/def2-TZVPP, G2,[23] G3,[24] G3B3,[25] and CCSD[26]/aug-cc-pVTZ. Results for these calculations are given in the Al_3H section below.

Electron Affinities. A variety of different single-point energy methods have been employed to determine total electronic energies for aluminum clusters, including numerous DFT functional combinations,[11−13,18] multi-reference CI (Al_n up to $n = 4$),[27] and coupled-cluster calculations (Al_n up to $n = 10$).[27] The coupled-cluster calculations of Ahlrichs and Drebov are of the highest quality and made use of a quadruple zeta quality basis set, which precluded using them on clusters larger than 10 atoms.[27] Paranthaman et al. used CCSD(T) single points at the def2-TZVPP geometries, also for clusters up to 10 aluminum atoms, in their study of electron affinities.[15]

We investigated several single-point energy methods in order to try to reproduce the adiabatic electron affinity of Al_3, which has been measured to be 1.92 eV.[28] The results of these calculations are shown in Table S1 of the Supporting Information. Raw electron affinities were computed by subtracting the zero-point energy-corrected energy (at 0 K) of the anionic cluster from that of the neutral cluster. The zero-point energy was obtained from the harmonic vibrational frequencies at the PBE0/def2-TZVPP geometry for each species and was not scaled. The raw electron affinity (EA) obtained from PBE0/def2-TZVPP calculations (126 basis functions, 207 primitive Gaussian functions for Al_3) on Al_3 and Al_3^- is 1.57 eV, which is underestimated by nearly 0.35 eV. Similar results were seen from raw EAs for Al_3 calculated with different functional combinations, B3LYP/def2-TZVPP and M06-2X/def2-TZVPP, as shown in Table S2. These methods also underestimate the EA of Al_3 by 0.36 and 0.37 eV, respectively. Even geometry optimizations using the CCSD/aug-cc-pVTZ method (Table S2) give an underestimated EA for Al_3 of 1.78 eV.

Given the success of single-point energy calculations at the CCSD(T) level in previous studies on aluminum clusters, we performed single-point energy calculations using the CCSD(T)/def2-TZVPP level of theory at the PBE0/def2-TZVPP geometries. The resulting EA of 1.75 eV is in better agreement with the experimental EA than the PBE0 value of 1.57, but it is still underestimated. It is perhaps not surprising that the electron affinities are underestimated for calculations using this basis set as diffuse functions are normally required for correct treatment of anions, and the def2-TZVPP basis set does not contain them. Incorporating diffuse functions into the basis set improves the results. The def2-TZVPPD basis set (144 basis functions, 228 primitive Gaussians) for aluminum was taken from the basis set exchange website,[29] and single-point energy calculations at the CCSD(T)/def2-TZVPPD//PBE0/def2-TZVPP level give an EA for Al_3 of 1.84 eV, which is still somewhat low. Re-optimizing both Al_3 and Al_3^- using the def2-TZVPPD basis set gives nearly identical geometries to those from the def2-TZVPP basis set, and the raw EA for Al_3 derived from the PBE0/def2-TZVPPD calculations was within 0.3 meV of the EA from the def2-TZVPP calculations (1.57 eV). Thus, including diffuse functions in the single-point energy calculations had a much larger effect on the derived EAs than on the optimized geometries, so we stayed with the def2-TZVPP basis set for geometry optimizations on the larger clusters.

Further increasing the basis set size of the CCSD(T) single-point energy calculation to Dunning's aug-cc-pVTZ basis set (150 basis functions, 345 primitive Gaussians)[30] gives an EA for Al_3 of 1.89 eV, in excellent agreement with the experimental EA. Interestingly, single-point energies at the CCSD(T)/aug-cc-pVTZ level at the B3LYP/def2-TZVPP, M06-2X/def2-TZVPP, and CCSD/aug-cc-pVTZ geometries lead to virtually identical derived EAs for Al_3 of 1.89, 1.88, and 1.89 eV, respectively (Table S2), in agreement with both the PBE0/def2-TZVPP computational result (1.89 eV) and the experimental EA (1.93 eV). All of these CCSD(T) calculations used the frozen core approach in which only the three valence electrons are used in the correlation calculation. We did perform CCSD(T)(Full)/aug-cc-pVTZ calculations on the Al_3 system at the PBE0 geometries, which lead to a raw electron affinity of 1.88 eV (Table S2), which is only 0.01 eV lower than the frozen core results. Frozen core CCSD(T) calculations were used for all subsequent calculations.

Realizing that the CCSD(T)/aug-cc-pVTZ single-point energy calculations would be quite expensive for the larger clusters, we tried less expensive PBE0/aug-cc-pVTZ single-point calculations at the PBE0/def2-TZVPP geometries, which gave an EA of 1.68 eV for Al_3. Thus, single-point energy calculations using both coupled-cluster methods and the Dunning augmented triple-zeta basis set were needed to reproduce the experimental EA for Al_3, and therefore, despite the cost, this method was used for all of the Al_n and Al_nH clusters. Total electronic energies at the PBE0/def2-TZVPP and CCSD(T)/aug-cc-pVTZ levels, zero-point energy corrections, and E_0 values for the lowest-energy structural isomer of all neutral and anionic Al_n and Al_nH clusters are given in Tables S4 and S5 of the Supporting Information.

The experimental EA values for Al_n ($n = 4−13$) were taken from the study of Li et al. using photoelectron spectroscopy at 193 nm.[31] In most of the recent computational literature on aluminum clusters, these are the experimental electron affinities to which computed EA values are compared[13−15,18] and are the recommended experimental values from a 2002 review by Schaefer III et al.[32] Despite this, the NIST webbook[33] lists the values from a photoelectron spectroscopy study by Kawamata et al.using the fourth harmonic of a Nd:YAG laser at 266 nm as the preferred values (and in their list of searchable EAs).[34] While their data are in accord with the study of Li et al. for $Al_3−Al_5$, for clusters $Al_6−Al_{13}$, their electron affinities are on average 0.28 eV lower than those of Li et al.'s study and are not in agreement with high-level calculations.[31] As an extreme example, Kawamata et al.'s EA for Al_{13} is 0.57 eV lower than Li et al.'s. Given the agreement of high-level calculations with the electron affinities from Li et al.,[13−15,18] we have chosen to use these values for our isodesmic approach (see below). Table 1 shows that the CCSD(T)/aug-cc-pVTZ//PBE0/def2-TZVPP approach gives a mean unsigned deviation of 0.08 eV for the raw calculated EAs compared to the literature electron affinities for Al_n with $n \leq 13$.[31] We expect that raw EAs for the aluminum hydride clusters should be of the same quality.

In addition to the raw EAs for the hydrides, we calculated isodesmic predictions for the electron affinities using eq 1. CCSD(T)/aug-cc-pVTZ single-point energy calculations were performed at the PBE0/def2-TZVPP geometries for all four species in eq 1, giving the relative EA between the aluminum

https://doi.org/10.1021/acs.jpca.1c10431
J. Phys. Chem. A 2022, 126, 1648−1659

Table 1. Derived Electron Affinities for Al_n and Al_nH at the CCSD(T)/aug-cc-pVTZ//PBE0/def2-TZVPP Level of Theory

Al_n	EA (raw)[a]	EA (expt)	Al_nH	EA (raw)[a]	EA (iso)[b]	EA (vertical)[c]
3	1.89	1.92[d]	3	1.66	1.69	1.69
4	2.33	2.20[e]	4	2.21	2.08	2.27
5	2.20	2.25[e]	5	1.94	1.99	2.07
6	2.54	2.63[e]	6	2.69	2.78	2.85
7	2.27	2.43[e]	7	1.87	2.03	2.10
8	2.12	2.35[e]	8	2.47	2.70	2.69
9	2.75	2.85[e]	9	2.50	2.60	3.07
10	2.56	2.70[e]	10	2.95	3.09	3.16
11	2.79	2.87[e]	11	2.45	2.53	2.74
12	2.71	2.75[e]	12	2.93	2.97	3.08
13	3.53	3.62[e]	13	2.69	2.78	3.22

[a]Raw electron affinity obtained from E_0 values for neutral at its optimized geometry and anion at its optimized geometry. [b]Isodesmic electron affinity obtained from E_0 values using reaction 1. [c]Vertical electron affinity obtained from E_0 values for neutral and anion both at the anion optimized geometry. [d]Ref 28. [e]Ref 31.

hydride cluster and its all-aluminum counterpart. This difference is combined with the experimental electron affinity to give an isodesmic prediction for the electron affinity of the hydride cluster, which is shown in Table 1.

$$Al_n + Al_nH^- \rightarrow Al_n^- + Al_nH \quad (1)$$

Vertical electron affinities were calculated by performing CCSD(T)/aug-cc-pVTZ single-point energy calculations on the neutral Al_nH clusters at the corresponding Al_nH^- geometry. The derived vertical EAs are also shown in Table 1.

RESULTS AND DISCUSSION

Al_nH (n = 3−6). Al_3 and Al_3^- both possess D_{3h} symmetry, so there is only one unique terminal position to place a hydrogen atom, as shown in Figure 1. For neutral Al_3H, this creates a molecule of C_{2v} symmetry (term in Figure S1), which is a minimum on the potential energy surface calculated at the PBE0/def2-TZVPP level. We explored two additional hydrogen placements, a C_{2v} structure with the hydrogen atom bridging two aluminum atoms in a plane (bridge) and a C_{3v}, face-centered arrangement with the hydrogen atom above the plane of the aluminum atoms (face). Interestingly, even for this relatively simple molecule, previous computational studies by Kawmaura et al.[35] and Loukhvitski et al.[36] disagree on the lowest-energy structure. Kawamura used B3LYP/6-311 + G* calculations and found that the "face-centered" isomer is ∼92 kJ/mol more stable than the "bridged isomer" but did not mention the terminal isomer.[35] In contrast, Loukhvitski et al. found that the terminal isomer was the lowest-energy isomer at the B97-2/aug-cc-pVTZ level of theory.[36] Figure S1 of the Supporting Information shows the three structures. At the PBE0/def2-TZVPP level of theory, the face-centered arrangement is the lowest-energy structural isomer (Figure 1), lying 4.0 kJ/mol lower than the terminal isomer and 64.9 kJ/mol lower than the bridged isomer. In addition to the PBE0/def2-TZVPP calculations, we optimized the geometries using the B3LYP/def2-TZVPP, M06-2X/def2-TZVPP, and CCSD/aug-cc-pVTZ methods. Table S3 shows that the face-centered arrangement is also the lowest-energy isomer at these levels. The C_{2v} terminal isomer is not a minimum at either the B3LYP/def2-TZVPP or M06-2X/def2-TZVPP levels. The hydrogen atom prefers a bent C_s geometry that lies 4.9 or 15.4 kJ/mol higher in energy than the face-centered arrangement (see Table S3), similar to the terminal structure for Al_3H^- (see discussion below and Figure 1 and Figure S1). The bridged isomer is also not a minimum at the B3LYP/def2-TZVPP or M06-2X/def2-TZVPP levels. All bridged structures either isomerize to the face-centered isomer or are transition states upon using the B3LYP and M06-2X functionals. We also performed CCSD/aug-cc-pVTZ geometry optimizations on the three Al_3H isomers and found the same energy ordering with the face-centered isomer having the lowest E_0 and the terminal and bridged isomers lying 2.9 and 68 kJ/mol higher in energy.

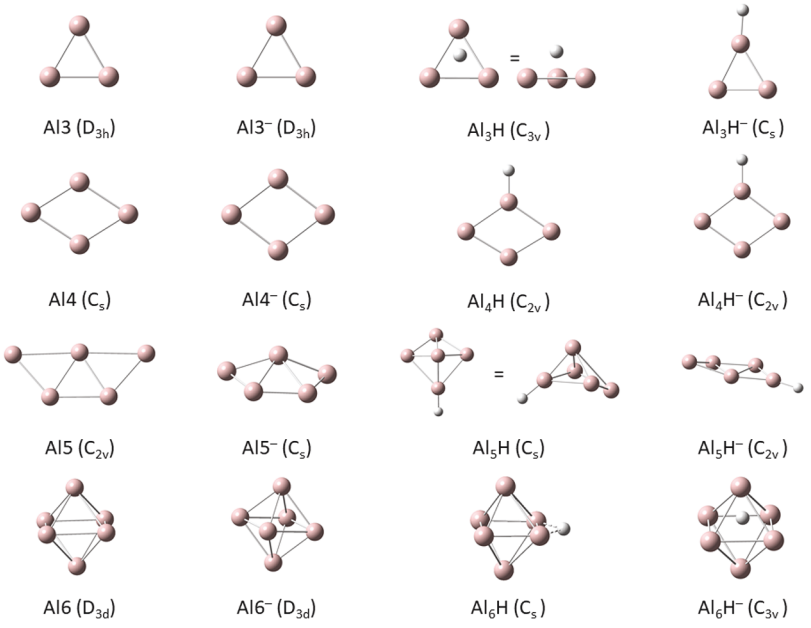

Figure 1. Lowest energy structures for Al_n, Al_n^-, Al_nH, and Al_nH^- (n = 3−6).

https://doi.org/10.1021/acs.jpca.1c10431
J. Phys. Chem. A 2022, 126, 1648−1659

CCSD(T)/aug-cc-pVTZ single-point energy calculations at the PBE0 geometries confirm that the face-centered and terminal isomers are very close in energy with an electronic energy difference of only 1.3 kJ/mol, which drops to a 0.9 kJ/mol 0 K energy difference when zero-point energy effects are considered. Similar differences (<2.0 kJ/mol) were obtained from CCSD(T) single-point energies using the B3LYP, M06-2X, and CCSD geometries as shown in Table S3.

In the Al_3H^- anion, the C_{2v} terminal structure is a transition state between two C_s structures at the PBE0/def2-TZVPP level. An IRC calculation was performed to locate the symmetry-related minima associated with the transition structure. One of these was re-optimized to obtain a final E_0 value for the terminal isomer. The optimized geometry has a distorted Al_3 arrangement with the hydrogen atom bent to give an H−Al−Al angle of ∼144° (Figure S1). Geometry optimization for the face-centered Al_3H^- isomer was performed starting in C_{3v} symmetry. After two optimization steps, the point group changed to C_1 and resulted in a "C_s-like" structure with two long Al−Al bonds (2.680 Å), one shorter Al−Al bond (2.491 Å), and the hydrogen atom ∼1.1 Å above the plane of the aluminum atoms. This structure is a transition state at the PBE0/def2-TZVPP level between two symmetry-related C_1 structures. An IRC calculation was performed to locate the associated minima, which were then re-optimized to give the final C_1 structure shown in Figure S1. The C_{2v}-bridged isomer is a minimum at the PBE0/def2-TZVPP level and is also shown in Figure S1. For the anion, the terminal isomer (term, Figure 1) has the lowest zero-point-corrected E_0 at the PBE0 level followed by the face-centered isomer (face) and the bridged isomer (bridge). CCSD(T) single-point energy-derived E_0 differences are +24.3 and + 29.1 kJ/mol for the face-centered and bridged isomers, respectively.

As with the neutrals, we investigated B3LYP/def2-TZVPP, M06-2X/def2-TZVPP, and CCSD/aug-cc-pVTZ geometries and found the same ordering of the three isomers (Table S3). CCSD(T)/aug-cc-pVTZ single-point energy calculations at these geometries give final differences in E_0 of 22.1, 23.2, and 22.7 kJ/mol between the terminal and face-centered isomers. The bridged isomer is the least stable isomer at the B3LYP and M06-2X geometries as well, with E_0 differences of 28.5 and 28.1 kJ/mol, respectively. We were unable to get the CCSD/aug-cc-pVTZ geometry calculations for the bridged anion to converge.

A raw adiabatic electron affinity for Al_3H was obtained from single-point energy calculations at the RCCSD(T)/aug-cc-pVTZ level for the face-centered isomer of Al_3H and at ROCCSD(T)/aug-cc-pVTZ for the terminal isomer of Al_3H^-, both at the PBE0/def2-TZVPP geometries. In each case, the unscaled zero-point energy from the PBE0/def2-TZVPP frequency calculations was added to the CCSD(T) electronic energy to give a 0 K energy E_0 (CCSD). A raw adiabatic electron affinity of 1.66 eV was obtained for Al_3H using the terminal anion and the face-centered neutral. We also calculated the RCCSD(T)/aug-cc-pVTZ single-point energy for the terminal neutral Al_3H, which leads to an adiabatic EA of 1.67 eV for terminal Al_3H to terminal Al_3H^-. Given the small size of this cluster and the good performance of the method in replicating the EA for Al_3, the raw EA should be quite accurate. However, there is a somewhat larger deviation in the calculated EAs for the larger clusters (see Table 1) compared to the experimental values. We therefore chose to also calculate isodesmic electron affinities for each hydride cluster using reaction 1. Using the experimental value of 1.92 eV for the EA of Al_3 gives isodesmic predictions of 1.69 eV for the adiabatic electron affinity for face-centered Al_3H and 1.70 eV for the terminal Al_3H, both to terminal Al_3H^-. Finally, a vertical electron detachment energy of 1.69 eV was obtained by performing a CCSD(T)/aug-cc-pVTZ calculation of neutral Al_3H at the optimized terminal Al_3H^- geometry.

Similar results were obtained from CCSD(T) calculations using the B3LYP, M06-2X, and CCSD geometries. Table S2 shows that both the raw and isodesmic EA values derived from these calculations differ by ≤0.02 eV. CCSD(T)(Full) single-point energy calculations were also carried out on all Al_3H/Al_3H^- isomers at the PBE0/def2-TZVPP geometries, and the derived raw and isodesmic electron affinities also differ by ≤0.02 eV from the frozen core calculations. We also investigated three of the QCISD(T)-based Gx methods, namely, G2, G3, and G3B3, as alternatives to the CCSD(T)-based approach. These methods overestimate the electron affinity of Al_3 by between 0.17 and 0.25 eV (Table S2) and give isodesmic electron affinities for Al_3H that are more than 0.24 eV smaller than the CCSD(T)-based methods. Due to their poor performance for Al_3/Al_3H and the computational cost of these methods for larger clusters, the Gx methods were not pursued further. Since the CCSD(T)/aug-cc-pVTZ single-point energy approach gives nearly identical derived electron affinities for Al_3H regardless of the method used for geometry optimization, this gives us confidence in using PBE0/def2-TZVPP geometries for the larger clusters.

Similar calculations were carried out for the larger aluminum hydride clusters. Isomer searches for Al_4H, Al_6H, and Al_7H found that the neutral and anionic clusters for these three hydrides have low-energy structures in which the arrangement of the aluminum atoms does not deviate greatly from that of their all-aluminum counterparts. In contrast, the lowest-energy conformers for both Al_5H and Al_8H and their anions have structures in which the aluminum atoms are in a different arrangement than in the all-aluminum clusters. Figure 1 shows the low-energy minima for the neutral and anionic all-aluminum clusters and their hydrides. Al_4 and Al_4^- are both diamond shaped with C_s symmetry, and Al_5 is a planar molecule with C_{2v} symmetry, whereas Al_5^- has a C_s structure in which the central atom is above the plane of the other four. Al_6 and Al_6^- are both distorted octahedra with D_{3d} symmetry. Al_7 and Al_7^- have C_{3v} structures in which the seventh aluminum atom is appended to one of the faces of Al_6 (Al_6^-).

For Al_4H, the lowest-energy structure at the PBE0 level is a C_{2v} terminal isomer (term1) with the hydrogen atom on the shorter axis of the diamond structure as shown in Figure 1 and Figure S2. For clusters with 4−6 aluminum atoms, our naming scheme denotes the position of the hydrogen (term, bridge, or face) and the relative ordering by CCSD(T)/aug-cc-pVTZ E_0, that is, term1 is the lowest-energy terminal structure and term2 is the next higher-energy terminal isomer. The terminal isomer with the hydrogen atom on the longer axis of the diamond (term2, Figure S2) is not a minimum on the C_{2v} surface but distorts to a C_s structure with a zero-point energy-corrected CCSD(T) energy difference of +32.2 kJ/mol compared to term1. A bridging isomer was also located +7.6 higher in CCSD(T) E_0. Placing a hydrogen atom in the face-centered position of neutral Al_4 results in a puckering of the aluminum atom framework and a C_{2v} structure that lies +9.5 kJ/mol in CCSD(T) E_0 above the term1 isomer. The relative energetics for the neutral clusters are consistent with the study of

https://doi.org/10.1021/acs.jpca.1c10431
J. Phys. Chem. A 2022, 126, 1648−1659

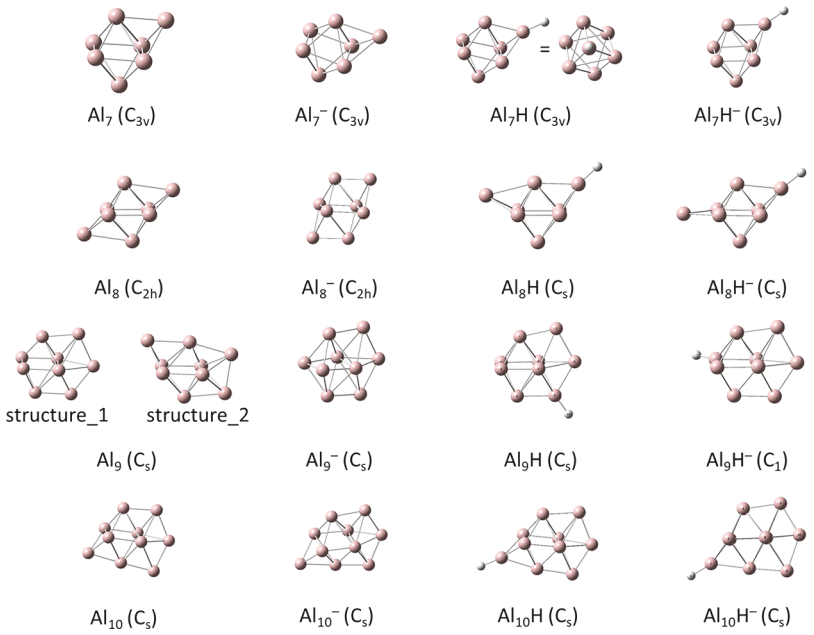

Figure 2. Lowest energy structures for Al_n, Al_n^-, Al_nH, and Al_nH^- (n = 7−10).

Loukhvitski et al. who also found the term1 structure as the global minimum at the B97-2/aug-cc-pVTZ level of theory.[36] Similar to the Al_3H case, Kawamura did not mention the terminal isomer but again listed the bridged isomer as the global minimum at the B3LYP/6-311 + G* level.[35]

For Al_4H^-, the relative ordering of the isomers is the same as for the neutral cluster with the term1 isomer as the ground state and the face, bridged, and term2 isomers lying 2.3, 12.6, and 50 kJ/mol higher in E_0 at the CCSD(T)/aug-cc-pVTZ level. The face-centered isomer for Al_4H^- is not puckered but has its aluminum atoms in a nearly square-planar arrangement with identical Al−Al bond lengths of 2.570 Å. A raw adiabatic electron affinity of 2.21 eV was calculated for Al_4H based on the term1 structures for Al_4H and Al_4H^-. An isodesmic adiabatic EA of 2.08 eV is derived relative to the experimental EA of Al_4 (2.20 eV), and a vertical EA of 2.27 eV is derived from CCSD(T) single-point energy calculations on Al_4H at the Al_4H^- term1 geometry. We also performed CCSD(T)(Full) single-point energy calculations on the Al_4H/Al_4H^- isomers, and the derived electron affinities were within 0.01 eV of the frozen-core calculations.

Placing a hydrogen atom onto Al_5 causes a distortion of the geometry of the aluminum atoms from the all-aluminum cluster. As shown in Figure 1 and Figure S3a, the lowest-energy conformer at the PBE0/def2-TZVPP level has the aluminum atoms in a pryamidal-like arrangement with the hydrogen attached terminally (term_pyr1). The terminal isomer in which the hydrogen atom is attached to the planar Al_5 structure (term1) is very close in energy lying 1.5 kJ/mol higher in E_0 at the CCSD(T)/aug-cc-pVTZ level. Additional higher-lying face-centered and bridging isomers (Figure S3a) were located lying 23.9 (face-pyr1), 27.8 (face1), 38.3 (bridge1), and 40.4 (bridge2) kJ/mol higher in E_0 at the CCSD(T) level. These results are in general agreement with Kawamura et al.'s previous study except for the relative stability of the two low-lying isomers (top and top-side in their nomenclature corresponding to term1 and term_pyr1 in ours).[35] They found that the planar arrangement was lower in energy than the tetrahedral-like arrangement at the B3LYP/6-311 + G* level, confirming that these two isomers are very close in energy.[35]

For the anionic Al_5H cluster, the two terminal isomers (term1 and term_pyr1) are again the lowest-energy isomers, but in this case, the term1 planar arrangement is lower in E_0 by 1.6 kJ/mol as shown in Figure 1 and Figure S3b. Eight additional isomers (Figure S3b) were located that lie between 18.7 and 43.0 kJ/mol above the global minimum structure. A raw EA for Al_5H of 1.94 eV is derived from the term1 isomer of Al_5H^- and the term_pyr1 isomer of Al_5H. An isodesmic adiabatic EA of 1.99 eV is derived based on the experimental EA for Al_5 of 2.25 eV. A vertical EA of 2.07 eV is derived from calculations of the neutral and anion at the term1 geometry.

Al_6 has a distorted octahedral D_{3d} structure, and placing a hydrogen atom on a terminal position causes the aluminum atoms to distort to a C_s structure (term) as shown in Figure S4. Placing a hydrogen atom in a bridging position between two aluminum atoms causes a similar but less drastic distortion of the structure, resulting in a bridged C_s structure (bridge, Figure S4). At the PBE0/def2-TZVPP level of theory, the C_{3v} face-centered isomer is a transition state between two C_s structures (face). The bridged isomer and the face-centered isomer were found to be very close in energy with the bridged structure lying 1.3 kJ/mol lower at the CCSD(T) single-point level. The terminal structure lies 34.1 kJ/mol above the bridged structure. These findings are in disagreement with the previous study of Kawamura et al. who does not mention the bridged structure or terminal isomers.[35]

For Al_6H^-, the C_{3v} face-centered arrangement is a minimum, and we were unable to locate any stable terminal or bridged isomers as all starting structures eventually isomerized to the face-centered isomer. A raw adiabatic EA of 2.69 eV was derived using the bridged neutral and face-centered anion. An isodesmic adiabatic electron affinity of 2.78 eV is derived using the experimental EA of 2.63 for Al_6. Finally, a vertical EA of 2.85 eV is derived from a calculation of the neutral Al_6H cluster at the Al_6H^- geometry.

Al_nH (n = 7−10). For Al_7, the preferred structure has a single aluminum atom appended to a face of the Al_6 cage.

https://doi.org/10.1021/acs.jpca.1c10431
J. Phys. Chem. A 2022, 126, 1648−1659

According to the "magic rule" model of Kiran et al.,[37] Al_7H with its hydrogen in a terminal arrangement on this "extra" atom should be a magic cluster with 20 "free" valence electrons according to the jellium model as the terminal arrangement of the hydrogen atom ties up its valence electron along with one of the electrons from the aluminum atom. The PBE0 method confirms that placement of a hydrogen atom terminally is preferred energetically (term7, Figure 2 and Figure S5). For clusters with seven or more aluminum atoms, our name scheme changed to indicate the position (terminal, bridging, or face) of the hydrogen atom relative to the atom numbers of the original all-aluminum clusters. Terminal isomers with hydrogens on the other aluminum atoms all rearranged back to the term7 structure or to a different structure (structure_2) in which the aluminum atoms have rearranged to a C_{2v} arrangement (term3_2). This isomer lies 12.8 kJ/mol higher in E_0 at the CCSD(T) level. Additional higher-lying isomers were located in which the hydrogen atom occupies one of two face-centered positions as shown in Figure S5. For the smaller clusters up to Al_6H, we performed CCSD(T)/aug-cc-pVTZ single-point energy calculations on all isomers we found in our conformer search to determine relative zero-point energy-corrected E_0 values at the CCSD(T) level. Due to the cost of CCSD(T) single-point energy calculations on the larger clusters, we only performed these calculations on selected low-energy isomers (generally within 20 kJ/mol of the global minimum structure as determined by PBE0 E_0 values) for Al_7H and larger clusters. The face-centered isomers for Al_7H are energetically disfavored, lying 95.6 and 109.6 kJ/mol above the term7 isomer in zero-point energy-corrected E_0 at the PBE0/def2-TZVPP level. Other isomers with the hydrogen bridging two aluminum atoms all collapsed to either the terminal or face-centered isomers during the optimization. This isomer ordering agrees with the results from the B3LYP study of Kawamura et al. in which they confirm that the terminal Al_7H molecule is "magic" with respect to its large HOMO-LUMO gap and significant decrease in binding energy for a second hydrogen atom.[35] Al_7H was included in a quantum Monte Carlo simulation of electron correlation effects in small aluminum hydride clusters by Damasceno et al., which also agrees that the terminal arrangement is the preferred isomer.[38]

Similarly in Al_7H^-, the terminal isomer is energetically favored over face-centered and bridging isomers as shown in Figure S5. A raw adiabatic EA of 1.87 eV is derived from the terminal isomers of the neutral and anionic clusters. An isodesmic EA of 2.03 eV is derived from the experimental EA of 2.43 eV for Al_8, and a vertical EA of 2.10 eV is derived from calculations of the neutral and anion at the anion geometry.

To our knowledge, this is the first study in which a systematic investigation of the structures of larger clusters $Al_8H-Al_{12}H$ has been carried out, so the results will be presented in more detail than those from previously studied clusters Al_3H-Al_7H and $Al_{13}H$. Al_8H is a second example of a hydride cluster in which the geometrical arrangement of the aluminum atoms changes from the all-aluminum cluster. Al_8 has a C_{2h} arrangement of atoms that is derived from the Al_6 scaffold in which the two additional aluminum atoms occupy opposite threefold symmetric face sites as shown in Figure 2. When an additional hydrogen atom is placed terminally on one of the "face" aluminum atoms, the other aluminum "face" atom migrates from the position opposite the terminal site on the other hemisphere of the cage to one that is on the opposite side but on the same hemisphere as shown in Figure 2 and Figure S6a (term1). Numerous attempts were made to locate terminal structures with the original Al_8 scaffold, but they all either isomerized to the term1 aluminum atom arrangement or were much higher in energy (see structure term4 in Figure S6a). Additional bridged and face-centered isomers were located lying between 24 and 64 kJ/mol higher in energy than the term1 structure and are also shown in Figure S6a. The lowest-energy conformer with the aluminum atoms in their Al_8 arrangement is a bridged structure lying 24.1 kJ/mol higher than the term1 isomer, whereas the lowest-energy face-centered isomer lies 51.6 kJ/mol higher in energy.

The lowest-energy isomer for Al_8H^- also has its hydrogen atom attached terminally to one of the "extra" aluminum atoms, which causes the other additional aluminum atom to migrate to the plane of the four aluminum atoms in the middle of the distorted octahedron (term1). Other higher-energy terminal isomers were located in which the aluminum atoms are in the original Al_8 arrangement (term4) or are no longer in a capped octahedral arrangement (term2). In addition, several bridged and face-centered isomers were located lying >45 kJ/mol above the term1 structure. The lowest lying bridged isomer is 45.6 kJ/mol less stable than term1, whereas the lowest-energy face-centered isomer lies 56.7 kJ/mol higher in energy. A raw adiabatic EA of 2.47 eV is derived from the term1 structures of the neutral and anion clusters. An isodesmic adiabatic EA of 2.70 eV is derived based on the experimental EA for Al_8 of 2.35 eV. A vertical EA of 2.69 eV is derived from calculations on the neutral and anionic clusters at the anion geometry.

Al_9 has a C_s structure that is again based on the Al_6 framework with the three additional aluminum atoms on the same side of the distorted octahedron as shown in Figure 2. We investigated several terminal, bridging, and face-centered placements of a hydrogen atom on this scaffolding, and low-energy structures within 65 kJ/mol of the global minimum isomer are shown in Figure S7a,b. In addition to those structures based on the lowest-energy Al_9 structure in Figure 1 (structure_1), we found several Al_9H cluster geometries based on a different arrangement of aluminum atoms that we will refer to as structure_2 (Figure 2). This isomer has two aluminum atoms on one side of the distorted octahedron and the third occupying a face-centered position on the other hemisphere. Despite the fact that this arrangement lies 24.2 kJ/mol in E_0 above structure_1 in the all-aluminum cluster at the PBE0/def2-TZVPP level, several Al_9H and Al_9H^- cluster geometries based on the structure_2 aluminum atom arrangement lie within 10 kJ/mol of their respective global minima. For Al_9H, the lowest-energy isomer is a terminal arrangement (term9) with the hydrogen atom on one of the "additional" aluminum atoms outside of the octahedral core. Placing the hydrogen atom on the ocatahedral core (term1 and term3) results in isomers lying 7.1 and 29.0 kJ/mol higher in E_0. Three terminal structure_2 isomers were located within 20 kJ/mol of the term9 isomer. For structure_2 isomers, the numbering scheme is different than for the structure_1 isomers and is based on the numbering of the aluminum atoms of structure_2. Additional higher-lying bridged and face-centered isomers based on the structure_1 and structure_2 arrangements were also located and are shown in Figure S7a,b. Interestingly, isomers with two additional aluminum atom arrangements were located that arose from starting geometries based on structure_1 and structure_2. These arrangements have the aluminum atoms in geometries that are based on the

https://doi.org/10.1021/acs.jpca.1c10431
J. Phys. Chem. A 2022, 126, 1648−1659

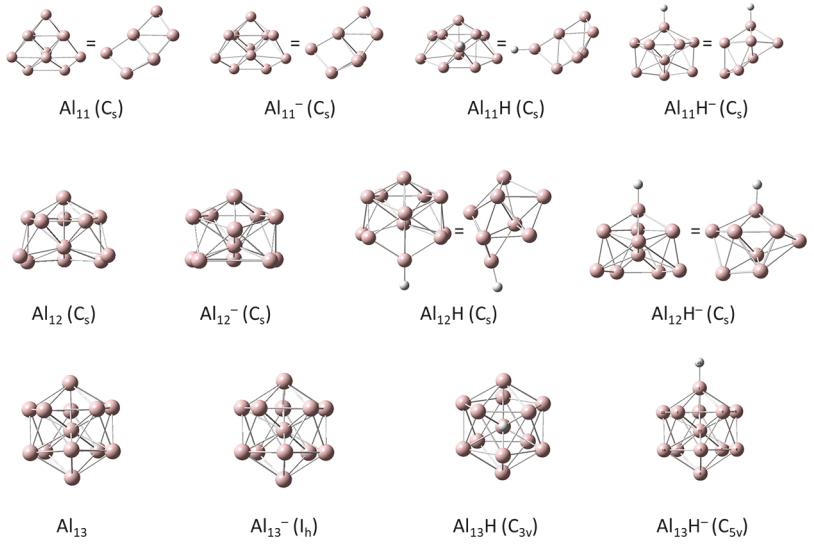

Figure 3. Lowest energy structures for Al_n, Al_n^-, Al_nH, and Al_nH^- (n = 11−13).

top part of an icosahedron in which a central atom is surrounded by rings of other aluminum atoms and a "capping" atom. As shown in Figure 2, as the size of the all-aluminum clusters increases, the most stable structures shift from the "octahedral" core of Al_6−Al_{10} toward icosahedral-like structures of Al_{11}−Al_{13} with such central atoms, rings, and capping atoms. Terminal and bridging isomers of structure_3 with a single capping atom were located 35.6 and 37.3 kJ/mol above term9, and terminal and bridging isomers of structure_4 with two capping atoms were located 46.5 and 61.2 kJ/mol above term9. CCSD(T) single-point energy calculations were performed on the four lowest-energy isomers and confirmed that the term9 isomer is the global minimum.

Similar results were found for Al_9H^-, except that the ordering of the term3 and term9 isomers switches, with term3 lying 5.0 kJ/mol lower in E_0 as shown in Figure S7c. A second term3 isomer was located with a compressed structure_1 arrangement in which the three "additional" atoms are significantly closer to the octahedral core, which lies 17.1 kJ/mol above the global minimum (term3b). The lowest-energy structure_2 isomer is a terminal arrangement (term7_2) that lies 17.8 kJ/mol above term3. Thirteen additional terminal, bridged, and face-centered structure_1 and structure_2 isomers were located with 75 kJ/mol of term3 and are shown in Figure S7c,d. In addition, structure_3 and structure_4 isomers were located lying >45 kJ/mol above term3. An adiabatic electron affinity of 2.50 eV was derived from the term9 isomer of Al_9H and the term3 isomer of Al_9H^-. Using the experimental EA of 2.85 eV for Al_9 gives an isodesmic adiabatic EA of 2.60 eV for Al_9H. A vertical EA of 3.07 eV is derived from a calculation of neutral Al_9H at the Al_9H^- term3 geometry.

Al_{10} has a structure that is based on the structure_1 Al_9 scaffold in which the additional aluminum atom is appended to a threefold face on the other hemisphere as shown in Figure 2. The $Al_{10}H$ isomer with the hydrogen atom appended to the "extra" hydrogen is the lowest-energy isomer at the PBE0 level (term1). Numerous higher-lying additional terminal, bridges, and face-centered isomers were located during an isomer search at the PBE0/3-21G level of theory as shown in Figure S8a. The term1 structure and the two next lowest-energy terminal isomers, term7 and term5, were re-optimized at the PBE0/def2-TZVPP level, and then CCSD(T) single-point energy calculations were performed to give relative 0 K energetics. Term7 and term5 isomers lie 16.5 and 34.0 kJ/mol higher in E_0 at the CCSD(T) level. All of the other terminal, bridged, and face-centered isomers lie at least 25 kJ/mol higher in energy at the PBE0/3-21G level. For the lowest-lying isomers, the arrangement of the aluminum atoms is nearly the same as for the all-aluminum clusters, but some of the higher-lying isomers show deviations from the all-aluminum cluster geometry.

Similar results were found for $Al_{10}H^-$ in which the lowest-energy isomer is also in a terminal arrangement as shown in Figure 2. We located 12 additional isomers in our PBE0/3-21G search, which are shown in Figure S8b. As with the neutral cluster, most of these isomers have an aluminum atom arrangement that is similar to that of the all-aluminum anionic cluster. We re-optimized the two lowest-energy isomers at the PBE/def2-TZVPP level and then performed CCSD(T) single-point energy calculations as with the other clusters to determine the relative E_0 for these two isomers. The term2 isomer lies 35.1 kJ/mol higher in E_0. All the other isomers had PBE0/3-21G energies of at least 45 kJ/mol higher than the term1 isomer. A raw adiabatic EA of 2.95 eV is derived from the term1 isomers of the neutral and anionic $Al_{10}H$ clusters. Using the experimental EA of 2.70 eV for Al_{10} provides an isodesmic adiabatic EA of 3.09 eV. Finally, a vertical EA of 3.16 eV is derived from calculations of the neutral and anion at the term1 anion geometry.

Al_nH (n = 11−13). For clusters larger than Al_{10}, the arrangement of the aluminum atoms includes one or more atoms on a central axis and multiple ring structures, which build toward the icosohedral arrangement of Al_{13}. For Al_{11}, the lowest-energy structure has a C_s structure shown in two aspects in Figure 3. A conformer search found 10 unique terminal, bridged, or face-centered isomers as shown in Figure S9a,b. At the PBE0/def2-TZVPP level, the lowest-energy structure has a terminal hydrogen placement (term7). Two additional terminal isomers (term11 and term8) were located with the aluminum atoms distorting from the Al_{11} scaffolding and lying 6.0 and 6.8 kJ/mol higher in energy. Seven high-lying bridged and face-centered arrangements were located that were >20 kJ/mol in E_0 above the term7 isomer. Most of these higher-

https://doi.org/10.1021/acs.jpca.1c10431
J. Phys. Chem. A 2022, 126, 1648−1659

lying isomers have aluminum atoms in an arrangement that is quite similar to that of the all-aluminum cluster. CCSD(T) single-point energies were calculated for the two lowest-energy isomers, and the final difference in E_0 is 9.9 kJ/mol with the term7 isomer lying lower.

Al_{11}^- has a similar aluminum atom arrangement to the corresponding neutral cluster. The two lowest $Al_{11}H^-$ isomers are terminal with isomer term1 having an aluminum atom scaffold similar to the all-aluminum cluster geometry and isomer term3 having a more icosahedral-based scaffold (Figure S9c). These two structures are very close in energy with a difference of 0.2 kJ/mol in E_0 at the PBE0/def2-TZVPP level and 2.7 kJ/mol at the CCSD(T) level. In both cases, the term3 isomer is lower in energy. A third terminal isomer, term11, has a geometry that corresponds to the term11 neutral $Al_{11}H$ cluster and lies 5.8 kJ/mol higher in E_0 at the PBE0/def2-TZVPP level. Eleven additional terminal and bridged isomers were located within 75 kJ/mol of the term3 isomer (Figure S9c,d). The aluminum atom arrangements in these clusters are all similar to the term 3 arrangement. A raw adiabatic electron affinity of 2.45 eV is derived for $Al_{11}H$ based on the term7 neutral and term3 anion. Using the experimental EA of 2.87 eV for Al_{11}leads to an isodesmic adiabatic EA of 2.53 eV for $Al_{11}H$. A vertical EA of 2.74 eV is derived from calculations of neutral $Al_{11}H$ at the term3 anion geometry.

Al_{12} has an icosahedral-like structure missing the bottom capping atom from the full icosahedral Al_{13} cluster as shown in Figure 3. In an icosahedron, the two five-membered rings are parallel, of the same size, and rotated 36° with respect to each other. In Al_{12}, the two rings are of different sizes, are eclipsed in rotation, and the bottom ring is tilted with respect to the axis of the top ring giving the molecule C_s symmetry that is actually closer in structure to a decahedron. Numerous terminal, bridged, and face-centered isomers were generated based on the Al_{12} scaffold and were optimized at the PBE0/def2-TZVPP level of theory. Fourteen minima were located within 70 kJ/mol of the lowest-energy structure. The four lowest-energy isomers at this level have terminal arrangements with varying distortions of the Al_{12} aluminum scaffold (Figure S10a,b). Two terminal isomers (term8 and term12) are essentially isoenergetic with term 1 and term3 isomers lying 6.5 and 11.0 kJ/mol higher in energy. The lowest-energy bridged structure is bridge18, which lies only 15 kJ/mol higher in E_0 at the PBE0/def2-TZVPP level, and the lowest-energy face-centered arrangement is face2-3-11, which lies 51.7 kJ/mol higher in energy. When CCSD(T) single-point energy calculations are carried out, the term1 isomer becomes the lowest energy structure by 3.3 kJ/mol over the term8 isomer, 6.1 kJ/mol over term12, and 14.6 kJ/mol over term3.

Al_{12}^- has a structure that is closer to a true icosahedral arrangement in which the two five-membered rings are staggered with respect to each other, though they are not planar, which gives the molecule C_s symmetry. Twelve terminal and bridged minima were located at the PBE0/def2-TZVPP level. The lowest-energy $Al_{12}H^-$ structure has a hydrogen atom on the top capping aluminum atom (term8a) of the cage structure. However, placing a hydrogen atom causes a significant rearrangement of the aluminum atoms in which one of the atoms from the bottom five-membered ring moves upward toward the top ring. Two views of this structure are shown in Figure 3 and Figure S10c. A second terminal isomer with the hydrogen atom on the top atom of the cage (term 6b) was located with a more severe distortion of the aluminum scaffold (term 8b), which lies 4.5 kJ/mol above term8a. Five additional terminal structures were located within 15 kJ/mol in E_0 of term8a. Each of these isomers has an aluminum atom arrangement that is subtly distorted from the all-aluminum anionic cluster. In addition to the terminal isomers, five bridged isomers were located, all of which lie greater than 22 kJ/mol higher in E_0. CCSD(T) single-point energy calculations were performed on the three lowest-energy terminal isomers, and term8a is still the lowest-energy structure by 6.4 and 12.1 kJ/mol over term1 and term8b, respectively. Using the term8a isomer for $Al_{12}H^-$ and the term1 isomer for $Al_{12}H$ leads to an adiabatic electron affinity of 2.93 eV. The experimental electron affinity of Al_{12} is 2.75 eV, which can be used to derive an isodesmic adiabatic EA of 2.97 eV. A vertical EA of 3.08 eV is derived from calculations of the neutral Al_{12} at the minimized Al_{12}^- geometry.

Al_{13} has a nearly icosahedral structure as shown in Figure 3. Due to the size and symmetry of the Al_{13} molecules, we only considered three $Al_{13}H$ isomers: terminal, bridged, and face-centered. These three isomers have been considered in detail in previous work by many different groups.[35,39−42] The most recent study is by Moc in which second-order Moller−Plessett perturbation theory was used for geometry optimizations and the determination of the nature of the stationary points.[43] CCSD(T) single-point energies were then used to determine the relative stability of the three minima types. They found that only the face-centered isomer is a minimum at the CCSD(T)/aug-cc-pVTZ//MP2/6-311++G(2d,2p) level of theory, whereas the terminal and bridged isomers are transition states that connect different face-centered minima. Moreover, the barrier for interconversion between face-centered sites was calculated to be only 10.9 kJ/mol, which suggests that the proton mobility across the surface of the cluster is high. These results were compared with DFT approaches using a number of different XC combinations including generalized gradient approximation (GGA: PBE, BP86), hybrid-GGA (PBE0, B3LYP), meta-GGA (TPSS), and hybrid-meta-GGA (M05-2X). They found that the terminal and bridged isomers are minima using density functional theory methods including PBE0 and that, in some cases, they lie lower in energy than the face-centered isomer.[43] Our results are in accord with this study and indicate that the bridged and face-centered isomers are extremely close in energy. At the PBE0/def2-TZVPP level of theory, the bridged isomer lies only 1.4 kJ/mol below the face-centered isomer in E_0, but this stability inverts at the CCSD(T)/aug-cc-pVTZ level with the face-centered isomer lying 2.4 kJ/mol lower in E_0 as shown in Figure 3 and Figure S11. The C_{5v} terminal isomer is a transition state at the PBE0/def2-TZVPP level, which connects two C_s-symmetry terminal isomers in which the hydrogen atom is tilted off of the C_5 axis. This isomer lies 23.1 kJ/mol above the face-centered isomer at the CCSD(T) level.

Al_{13}^- has a perfect icosahedral structure and with 40 electrons is considered a magic cluster with a filled shell according to the jellium model. Moc also studied the $Al_{13}H^-$ cluster and, in contrast to the neutral, found that the C_{5v} terminal structure is the global minimum at all levels studied.[43,44] Our results are in accord with those of Moc's in which we find that the terminal isomer (Figure 3 and Figure S11) lies 72 kJ/mol lower in energy than the C_{3v} face-centered isomer at the PBE0/def2-TZVPP level. The C_{2v} bridged isomer is a transition state at this level connecting two terminal isomers.

https://doi.org/10.1021/acs.jpca.1c10431
J. Phys. Chem. A 2022, 126, 1648−1659

Negative ion photoelectron spectroscopy (NIPES) experiments were performed on $Al_{13}H^-$ by Burkart et al., and they found three peaks in the spectrum at electron binding energies of 2.2, 3.8, and 4.3 eV.[45] The difference of around 1.6 eV between the two low-energy peaks is an estimate of the HOMO-LUMO gap and indicates that neutral $Al_{13}H$ is very stable. $Al_{13}H$ has 40 valence electrons similar to Al_{13}^- and is a closed-shell molecule according to the jellium model, which is in agreement with the large HOMO-LUMO gap found in the PES experiment. A similar experiment was performed by Grubisic et al. in which they were able to measure electron binding energies for two different $Al_{13}H^-$ isomers.[42] One of these (isomer A, the spectrum of which matches that of the Burkhart study) was determined to be a metastable species with a vertical detachment energy of 2.2 eV. The other (isomer B) is a more thermodynamically stable species with a vertical detachment energy of 3.15 eV and was not observed in the Burkhart study. By careful varying of the timing between cluster formation in the source and the photo-detachment pulse, they were able to record the spectra that allowed for the separation of the contributions of the two isomers. Through a comparison with calculations, they assigned the metastable isomer A to the face-centered isomer of $Al_{13}H^-$ and the more stable isomer B to be the terminal isomer. Our computed EA values are in accord with these findings[42] and with the theoretical study of Moc.[44] A vertical EA of 3.22 eV is derived for the terminal isomer of Al_3H at the CCSD(T) level, in excellent agreement with the 3.15 eV feature from the PES spectrum. A raw adiabatic EA of 2.69 eV is derived using the face-centered isomer of $Al_{13}H$ and the terminal isomer of $Al_{13}H^-$. Using the experimental EA of Al_{13} of 3.62 eV leads to an isodesmic adiabatic EA of 2.78 eV, which is somewhat larger than the adiabatic EA of 2.63 listed in the Grubisic study[42] but is in excellent agreement with the 2.80 eV thermodynamic EA value of Moc.[43]

Trends. The electron affinities for the all-aluminum clusters alternate from high to low beginning with Al_9. Results from photoelectron spectroscopy[31] indicate that signatures from *s* and *p* shells begin to overlap at $n = 9$, and *s*-*p* hybridization is evident in clusters larger than $n = 9$. They point out that such hybridization of *s* and *p* electrons is a requirement for bulk-like behavior in larger clusters. Even-numbered neutral all-aluminum clusters are ground-state singlets and have relatively smaller electron affinities, and odd-numbered clusters are ground-state doublets with relatively higher EAs. In our previous variable-temperature kinetic study of the reaction of Al_n^- ($n = 3-17$) with O_2, we showed that experimentally derived Arrhenius parameters can be rationalized by an early barrier involving long-range electron transfer to the O_2 molecule, similar to surface oxidation of bulk aluminum.[5−7] In addition, we showed that the derived activation barriers track the experimental electron affinities for clusters greater than $n = 9$. Even-numbered clusters with low electron affinities have a lower barrier at the initial electron transfer to O_2 and vice versa with the odd-numbered clusters.

Our results for Al_nH clusters indicate that the trends reverse with odd-numbered clusters now having the relatively lower electron affinities. This is consistent with the addition of a hydrogen atom changing the overall spin of the cluster. Comparison of the previously measured barriers for Al_nH^- ($n = 3,4,10-12$) with the presently calculated EAs is shown in Figure 4. Clusters of $n = 10-12$ all fit well with the linear fit for $n \geq 9$, while those of $n = 3$ and 4 deviate. This suggests that there is an increased *s*-*p* hybridization for $n = 10-12$, making them more akin to bulk and the primary perturbation of H being a change in spin. For the smaller clusters, this is not the case, and the calculated electron affinities of Al_nH^- tend to mirror the Al_n^- cluster as opposed to the Al_{n+1}^-.

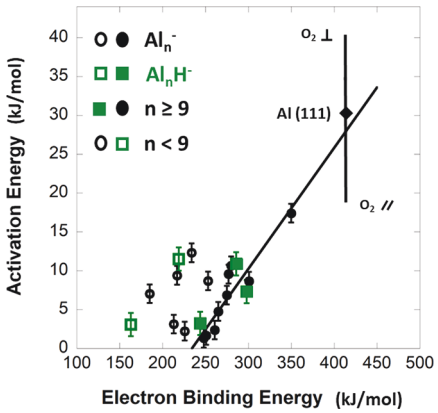

Figure 4. Experimentally derived activation energies for oxidation of Al_n^- (black circles, as published in ref 5 and Al_nH^- (green squares) clusters as a function of electron binding energy. The barrier for bulk Al (111) as calculated in ref 7 as a function of the aluminum bulk work function is also shown.

CONCLUSIONS

Adiabatic and vertical electron affinities for Al_nH clusters with $n = 3-13$ have been derived from coupled-cluster calculations at density functional theory-optimized geometries. Structures with terminal, bridging, and face-centered placements were investigated for each neutral and anionic clusters. The identities and relative energetics of the different isomers for clusters with $n = 3-8$ and 13 are in excellent agreement with previous literature studies. This gives us confidence that the CCSD(T)/aug-cc-pVTZ//PBE0/def2-TZVPP method is appropriate for such studies on clusters with $n = 9-12$, for which this is the first comprehensive study of the relative energetics of different isomers.

Derived adiabatic electron affinities for Al_nH show an even-odd alternation with even-numbered clusters having relatively larger EAs than odd-numbered clusters. The relationship between the presently calculated electron affinities and the previously observed Arrhenius barrier in the reaction with O_2 is consistent between Al_n^- and Al_nH^- for $n \geq 9$, suggesting a common mechanism by which reactivity is limited by a long-range charge transfer from the anion to O_2. This more bulk-like behavior suggests that *s*-*p* hybridization becomes prominent in a similar size regime for both the Al_n^- and Al_nH^- clusters.

ASSOCIATED CONTENT

Supporting Information

The Supporting Information is available free of charge at https://pubs.acs.org/doi/10.1021/acs.jpca.1c10431.

(I) Derived electron affinities for Al_3 at different levels of theory, electron affinities (eV) for Al_3 and Al_3H calculated with different methods, relative zero-point-corrected energies (kJ/mol) for Al_3H and Al_3H^- clusters calculated with different methods, and total electronic energies, zero-point energies, and E_0 values for Al_n ,Al_n^-, Al_nH, and Al_nH^- (Tables S1−S5); cartesian coordinates

https://doi.org/10.1021/acs.jpca.1c10431
J. Phys. Chem. A 2022, 126, 1648−1659

for the lowest energy structures for Al_nH and Al_nH^- (n = 3−13); (III) low-energy structures and relative energetics for Al_nH and Al_nH^- (n = 3−13) (Figures S1−S11) (PDF)

AUTHOR INFORMATION

Corresponding Author

John C. Poutsma − *Department of Chemistry, The College of William and Mary, Williamsburg, Virginia 23187-8795, United States;* orcid.org/0000-0002-0085-4079; Email: jcpout@wm.edu

Authors

William Moeller − *Department of Chemistry, The College of William and Mary, Williamsburg, Virginia 23187-8795, United States*

Jennifer L. Poutsma − *Department of Chemistry and Biochemistry, Old Dominion University, Norfolk, Virginia 23529, United States*

Brendan C. Sweeny − *Institute for Scientific Research, Boston College, Chestnut Hill, Massachusetts 02467, United States*

Shaun G. Ard − *Air Force Research Laboratory, Space Vehicles Directorate, Kirtland Air Force Base, Albuquerque, New Mexico 87117, United States*

Albert A. Viggiano − *Air Force Research Laboratory, Space Vehicles Directorate, Kirtland Air Force Base, Albuquerque, New Mexico 87117, United States*

Nicholas S. Shuman − *Air Force Research Laboratory, Space Vehicles Directorate, Kirtland Air Force Base, Albuquerque, New Mexico 87117, United States;* orcid.org/0000-0002-0274-2644

Complete contact information is available at: https://pubs.acs.org/10.1021/acs.jpca.1c10431

Notes

The authors declare no competing financial interest.

ACKNOWLEDGMENTS

Funding for this project was generously provided by the Air Force Office of Scientific Research (AFOSR-19RVCOR042), the Air Force Summer Faculty Fellowship Program (J.L.P. and J.C.P.), and the National Science Foundation (CHE1800137) (J.L.P. and J.C.P.).

REFERENCES

(1) Jarrold, M. F.; Bower, J. E.; Kraus, J. S. Collision induced dissociation of metal cluster ions: Bare aluminum clusters, Al^{+n} (n=3−26). *J. Chem. Phys.* **1987**, *86*, 3876.

(2) Leuchtner, R. E.; Harms, A. C.; Castleman, A. W., Jr. Aluminum Cluster Reactions. *J. Chem. Phys.* **1991**, *94*, 1093.

(3) Knight, W. D.; Clemenger, K.; de Heer, W. A.; Saunders, W. A.; Chou, M. Y.; Cohen, M. L. Electronic Shell Structure and Abundances of Sodium Clusters. *Phys. Rev. Lett.* **1984**, *52*, 2141.

(4) Burgert, R.; Schnöckel, H.; Grubisic, A.; Li, X.; Stokes, S. T.; Bowen, K. H.; Ganteför, G. F.; Kiran, B.; Jena, P. Spin Conservation Accounts for Aluminum Cluster Anion Reactivity Pattern with O_2. *Science* **2008**, *319*, 438.

(5) Sweeny, B. C.; McDonald, D. C., II; Poutsma, J. C.; Ard, S. G.; Viggiano, A. A.; Shuman, N. S. Redefining the Mechanism of O_2 Etching of Al_n^- Super Atoms: An Early Barrier Controls Reactivity, Analogous to Surface Oxidation. *J. Phys. Chem. Lett.* **2020**, *11*, 217.

(6) Libisch, F.; Huang, C.; Liao, P.; Pavone, M.; Carter, E. A. Origin of the Energy Barrier to Chemical Reactions of O_2 on Al(111): Evidence for Charge Transfer, Not Spin Selection. *Phys. Rev. Lett.* **2012**, *109*, 198303.

(7) Yin, R.; Zhang, Y.; Libisch, F.; Carter, E. A.; Guo, H.; Jiang, B. Dissociative Chemisorption of O_2 on Al(111): Dynamics on a Correlated Wave-Function-Based Potential Energy Surface. *J. Phys. Chem. Lett.* **2018**, *9*, 3271.

(8) Frisch, M. J.; Trucks, G. W.; Schlegel, H. B.; Scuseria, G. E.; Robb, M. A.; Cheeseman, J. R.; Scalmani, G.; Barone, V.; Mennucci, B.; Petersson, G. A.; et al. *Gaussian 09*; *Revision E.01* E. 01 Gaussian, Inc.: Wallingford, CT, 2013.

(9) Frisch, M. J.; Trucks, G. W.; Schlegel, H. B.; Scuseria, G. E.; Robb, M. A.; Cheeseman, J. R.; Scalmani, G.; Barone, V.; Petersson, G. A.; Nakatsuji, H.; et al. *Gaussian 16 Rev. C.01* Wallingford, CT 2016.

(10) Purvis, G. D., III; Bartlett, R. J. A Full Coupled-Cluster Singles and Doubles Model − the Inclusion of Disconnected Triples. *J. Chem. Phys.* **1982**, *76*, 1910.

(11) Chuang, F. C.; Wang, C. Z.; Ho, K. H. Structure of Neutral Aluminum Clusters Al_n 2 < n < 23: Genetic Algorithm Tight-Binding Calculations. *Phys. Rev. B* **2006**, *73*, 125431.

(12) Drebov, N.; Ahlrichs, R. Structures of Al_n, its Anions and Cations up to n = 34: A Theoretical Investigation. *J. Chem. Phys.* **2010**, *132*, 164703.

(13) Candidio, L.; Teixeira-Rabelo, J. N.; Da Silva, J. L. F.; Hai, G.-Q. Quantum Monte Carlo Study of Small Aluminum Clusters Al_n (n = 2−13). *Phys. Rev. B* **2012**, *85*, 245404.

(14) Kiohara, V. O.; Carvalho, E. F. V.; Paschoal, C. W. A.; Machado, F. B. C.; Roberto-Neto, O. DFT and CCSD(T) Electronic Properties and Structures of Aluminum CLusters: Al_n^x (n = 1-9, x = 0 ±1). *Chem. Phys. Lett.* **2013**, *568-569*, 42.

(15) Paranthaman, S.; Hong, K.; Kim, J.; Kim, D. E.; Kim, T. K. Density Functional Theory Assesment of Molecular Structures and Energies of Neutral and Anionic Al_n (n = 2-10) Clusters. *J. Phys. Chem. A* **2013**, *117*, 9293.

(16) Adamo, C.; Barone, V. Toward Reliable Density Functional Methods Without Adjustable Parameters: The PBE0 Method. *J. Chem. Phys.* **1999**, *110*, 6158.

(17) Weigend, F.; Alrichs, R. Balanced Basis Sets of Split Valence, Triple Zeta Valence and Quadruple Zeta Valence Quality for H to Rn: Design and Assessment of Accuracy. *Phys. Chem. Chem. Phys.* **2005**, *7*, 3297.

(18) Rao, B. K.; Jena, P. Evolution of the Electronic Structure and Properties of Neutral and Charged Aluminum Clusters: A Comprehensive Analysis. *J. Chem. Phys.* **1999**, *111*, 1890.

(19) Gordon, M. S.; Binkley, J. S.; Pople, J. A.; Pietro, W. J.; Hehre, W. J. Self-Consistent Molecular Orbital Methods. 22. Small Split-Valence Basis Sets for Second-Row Elements. *J. Am. Chem. Soc.* **1982**, *104*, 2797.

(20) Becke, A. D. Density Functional Thermochemistry. III. The Role of Exact Exchange. *J. Chem. Phys.* **1993**, *98*, 5648.

(21) Lee, C.; Yang, W.; Parr, R. G. Development of the Colle-Salvetti Correlation Energy Formula into a Functional of the Electron Density. *Phys. Rev. B* **1988**, *37*, 785.

(22) Zhao, Y.; Trular, D. G. The M06 Suite of Density Functionals for Main Group Thermochemistry, Thermochemical Kinetics, Noncovalent Interactions, Excited States, and Transition Elements: Two New Functionals and Systematic Testing of Four M06-class Functionals and 12 Other Functionals. *Theor. Chem. Acc.* **2008**, *120*, 215.

(23) Curtiss, L. A.; Raghavachari, K.; Trucks, G. W.; Pople, J. A. Gaussian-2 Theory for Molecular Energies of First- and Second-Row Compounds. *J. Chem. Phys.* **1991**, *94*, 7221.

(24) Curtiss, L. A.; Raghavachari, K.; Redfern, P. C.; Rassolov, V.; Pople, J. A. Gaussian-3 (G3) Theory for Molecules Containing First and Second Row Atoms. *J. Chem. Phys.* **1998**, *109*, 7764.

(25) Baboul, A. G.; Curtiss, L. A.; Redfern, P. C.; Raghavachari, K. Gaussian-3 Theory Using Density Functional Geometries and Zero-point Energies. *J. Chem. Phys.* **1999**, *96*, 1218.

(26) Scuseria, G. E.; Janssen, C. L.; Schaefer, H. F., III An Efficient Reformulation of the Closed-Shell Coupled Cluster Single and Double Excitation (CCSD) Equations. *J. Chem. Phys.* **1988**, *89*, 7382.
(27) Drebov, N.; Ahlrichs, R. Small Clusters of Aluminum and Tin: Highly Correlated Calculations and Validation of Density Functional Procedures. *J. Chem. Phys.* **2011**, *134*, 124308.
(28) Villalta, P. W.; Leopold, D. G. A Study of the Ground and Excited States of Al_3 and Al_3^-. I. 488 nm Anion Photoelectron Spectrum. *J. Chem. Phys.* **2009**, *130*, No. 024303.
(29) Pritchard, B. P.; Altarawy, D.; Didier, B.; Gibson, T. D.; Windus, T. L. New Basis Set Exchange: An Open, Up-to-date Resource for the Molecular Sciences Community. *J. Chem. Inf. Model.* **2019**, *59*, 4814.
(30) Woon, D. E.; Dunning, T. H., Jr. Gaussian Basis Sets for Use in Correlated Molecular Calculations. III. The Atoms Aluminum Through Argon. *J. Chem. Phys.* **1993**, *98*, 1358.
(31) Li, X.; Hongbin, W.; Wang, X.-B.; Wang, L.-S. s-p Hybridization and Electron Shell Structures in Aluminum Clusters: A Photoelectron Spectroscopy Study. *Phys. Rev. Lett.* **1998**, *81*, 1909.
(32) Rienstra-Kiracofe, J. C.; Tschumper, G. S.; Schaefer, H. F., III; Ellison, G. B. Atomic and Molecular Electron Affinities: Photoelectron Experiments and Theoretical Computations. *Chem. Rev.* **2002**, *102*, 231.
(33) Bartmess, J. E. *Negative Ion Energetics Data In NIST Chemistry WebBook, NIST Standard Reference Database Number 69*; Mallard, W. G.; Linstrom, P. J. Ed.; National Institute of Standards and Technology: Gaithersburg MD, 20899, 2018.
(34) Kawamata, H.; Negishi, Y.; Nakajima, A.; Kaya, K. Electronic Properties of Substituted Aluminum Clusters by Boron and Carbon Atoms ($Al_nB_m^-/Al_nC_m^-$); New Insights into s-p Hybridization and Perturbed Shell Structures. *Chem. Phys. Lett.* **2001**, *337*, 255.
(35) Kawamura, H.; Kumar, V.; Sun, Q.; Kawazoe, Y. Magic Behavior and Bonding Nature in Hydrogenated Aluminum Clusters. *Phys. Rev. B* **2001**, *65*, No. 045406.
(36) Loukhovitski, B. I.; Torokhov, S. A.; Loukhovitskaya, E. E.; Sharipov, A. S. DFT Study of Small Aluminum and Boron Hydrides: Isomeric Composition and Physical Properties. *Struct. Chem.* **2018**, *29*, 49.
(37) Kiran, B.; Jena, P.; Li, X.; Grubisic, A.; Stokes, S. T.; Ganteför, G.; Bowen, K. H.; Burgert, R.; Schnöckel, H. Magic Rule for Al_nH_m Magic Custers. *Phys. Rev. Lett.* **2007**, *98*, 256802.
(38) Damasceno, J. H., Jr.; Teixeira Rabelo, J. N.; Candido, L. A Quantum Monte Carlo Study of Electron Correlation Effects in Small Aluminum Hydride Clusters. *New J. Chem.* **2015**, *39*, 2195.
(39) Khanna, S. N.; Jena, P. Reactivity of Hydrogen With Open and Closed Shell Clusters. *Chem. Phys. Lett.* **1994**, *218*, 383.
(40) Henry, D. J.; Varano, A.; Yarovsky, I. Performance of Numerical Basis Set DFT for Aluminum Clusters. *J. Phys. Chem. A* **2008**, *112*, 9835.
(41) Han, Y.-K.; Jung, J.; Kim, K. H. Structure and Stability of $Al_{13}H$ clusters. *J. Chem. Phys.* **2005**, *122*, 124319.
(42) Grubisic, A.; Li, X.; Stokes, S. T.; Vetter, K.; Gantefoer, G.; Bowen, K.; Jena, P.; Kiran, B.; Burgert, R.; Schnoeckel, H. $Al_{13}H^-$: Hydrogen Atom Site Selectivity and the Shell Model. *J. Chem.Phys.* **2009**, *131*, 121103.
(43) Moc, J. The electron affinity of the $Al_{13}H$ cluster: high level *ab initio* study. *Mol. Phys.* **2014**, *112*, 2781.
(44) Moc, J. Ab Initio Correlated Study of the $Al_{13}H^-$ Anion: Isomers, Their Kinetic Stability and Vertical Detachment Energies. *Chem. Phys. Lett.* **2012**, *521*, 12.
(45) Burkart, S.; Blessing, N.; Klipp, B.; Miller, J.; Gantefoer, G.; Seifert, G. Experimental Verification of the High Stability of $Al_{13}H$: a Building Block of a New Type of Cluster Material? *Chem. Phys. Lett.* **1999**, *301*, 546.

https://doi.org/10.1021/acs.jpca.1c10431
J. Phys. Chem. A 2022, 126, 1648−1659